Metal plate for guiding terahertz surface plasmon-polaritons and its sensing applications

Liu, J; Liang, H; Zhang, M; Su, H

Metal plate for guiding terahertz surface plasmon-polaritons and its sensing applications

Jiamin Liu[a, b, c], Huawei Liang[a, b, c]*, Min Zhang[a, b, c], and Hong Su[a, b, c]

[a]College of Electronic Science and Technology, Shenzhen University, Shenzhen, 518060, China
[b]Shenzhen Key Laboratory of Laser Engineering, Shenzhen University, Shenzhen, 518060, China
[c]Key Laboratory of Advanced Optical Precision Manufacturing Technology of Guangdong Higher Education Institutes, Shenzhen University, Shenzhen, 518060, China *Corresponding author: hwliang@szu.edu.cn

Abstract: We report the guiding of THz surface plasmon-polaritons using metal plates. We theoretically study the transmission characteristics of the bare and dielectric coated metal plate and compared the difference between them. We propose coupling the THz SPPs on a bare metal plate using single dielectric film, and the highest theory coupling efficiency we get can be 45.64%. Moreover we study the hybrid plasmonic modes of a dielectric slab above the metal plate, and we find that the THz SPPs on metal plate is strongly affected by the dielectric slab. We further discuss the interesting phenomenon of the transmission spectrum influenced by the variation of air interval between the dielectric slab and metal plate.

Key words: Waveguides ; Infrared, far; Waveguides, planar

1. Introduction

THz waveguides have been widely studied in recent years, such as cylindrical wire waveguides [1], low-index THz pipe waveguides [2] and planar wire waveguides [3]. Since they are first proposed, there are many similar THz waveguides [4-7] have been studied, and many interesting theoretical and experimental conclusions have been given. THz waveguides have been widely used in communications, spectroscopy, imaging, detection and sensing [8-11]. The sensing of the thin dielectric film on the cylindrical metal wires are reported by several articles [10,11]. There are also several articles report the THz surface plasmon-polaritons (THz SPPs) on single metal plate [12-14], and the sensing of dielectric film on single metal plate surface has also been discussed [13,14]. Although similar results have been given on coated or uncoated metal plates waveguide, the theory has not been given exclusively yet. And even though the coupling efficiency is increased much after coating the metal plate, the coupling efficiency to bare metal plate is extremely low [12]. Moreover the hybrid plasmonic modes [15,16] of a dielectric slab above the metal plate is not discussed yet.

In this paper, we report the guiding of THz SPPs using metal plates. We theoretically study the transmission characteristics of the bare and dielectric coated metal plate and compared the difference between them. We propose coupling the THz SPPs on bare metal plate using single dielectric film, and the highest theory coupling efficiency we get can be 45.64%. Then we study the hybrid plasmonic modes of a dielectric slab above the metal plate, and we find that the THz SPPs on metal plate is strongly affected by the dielectric slab. We further discuss the interesting phenomenon of the transmission spectrum influenced by the variation of the air interval between the dielectric slab and metal plate. We believe that these results are very useful for sensing applications of THz SPPs on metal plate.

2. THz SPPs on metal plate

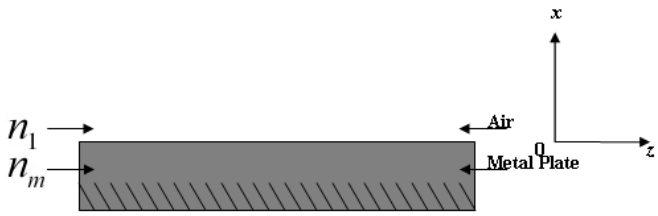

Fig.1 Metal plate structure and the coordinate system

The structure of metal plate is shown in Fig. 1, x = 0 plane is on the metal interface, and the waveguide width in y direction is infinity. When transverse magnetic (TM) modes propagate in positive z-direction, the field components can be written as [17]:

$$H_y(x) = \begin{cases} Ae^{-h_1 x} & x \geq 0 \\ Ae^{h_m x} & x \leq 0 \end{cases} \quad (1)$$

where A is a coefficient related with the mode power; $h_1 = (\beta^2 - n_1^2 k_0^2)^{1/2}$, $h_m = (\beta^2 - n_m^2 k_0^2)^{1/2}$; n_1 and n_m are refractive index of air and metal, respectively. $\beta = \beta_1 - i*\alpha$ is the propagation constant of the guiding mode, in which the real part β_1 is related to the effective refractive index $n_{eff} = \beta_1 / k_0$ and the

imaginary part α is the loss coefficient of the mode. k_0 is the wave vector in vacuum.

The dispersion equation of TM mode can be represented as [7] :

$$\beta = \sqrt{\frac{\varepsilon_m \varepsilon_1}{\varepsilon_1 + \varepsilon_m}} k_0 \qquad (2)$$

$\varepsilon_1 = n_1^2$ and $\varepsilon_m = n_m^2$ are the relative permittivity of air and metal plate respectively. Copper is used as the material for metal plate, and the relative permittivity can be obtained according to Drude model:

$$\varepsilon_m = \varepsilon_\infty - \frac{\omega_p^2}{\omega^2 - j\omega\omega_\tau} \qquad (3)$$

where ω is the angular frequency of the THz wave, ε_∞ is the high frequency permittivity of copper, which is always negligible in the THz region. $\omega_p = 1.1234 \times 10^{16}$ Hz and $\omega_\tau = 1.3798 \times 10^{13}$ Hz are the plasma oscillation frequency and damping frequency of copper [18], respectively.

By Eq.(2), we calculate the dependence of the loss on THz frequency and present the corresponding effective refractive index as shown in Fig. 2:

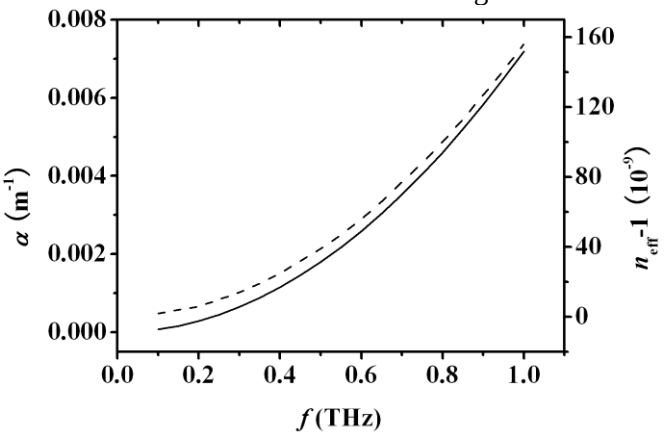

Fig. 2 Loss (solid line) and effective refractive index (dashed line) of metal plate THz SPPs as a function of THz frequency

Figure 2 illustrates that the loss increases with the increase of frequency, and it is very low. For the regime of less than 1 THz, the loss is lower than $0.008m^{-1}$ which is two orders of magnitude lower than the loss of cylindrical wire THz SPPs. However, the effective refractive index is closer to 1 than that of cylindrical wire, and $n_{eff} - 1$ is in the magnitude of 10^{-9}, which means the dispersion is much lower and the mode field radius is much larger.

By Eq. (1), we get the mode field distribution of the metal plate at 1 THz, as shown in Fig. 3:

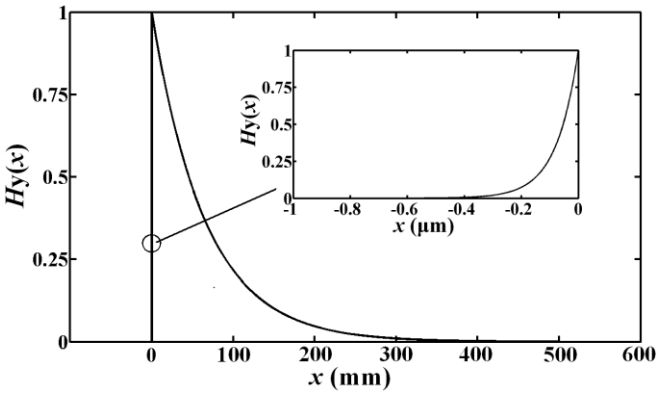

Fig.3 Mode field distribution of metal plate THz SPPs at 1THz. Inset shows the mode field distribution in the metal

Figure 3 illustrates that the field amplitude of metal plate mode is still very strong at 200 mm in the air. However, the THz wave transmits through 0.2 μm in metal only.

3. Sensing applications of metal plate

3.1 The sensing of dielectric film on metal plate

The dielectric cladding metal plate structure is shown in Fig. 4:

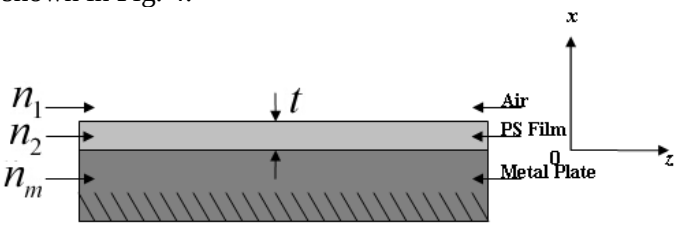

Fig.4 Dielectric cladding metal plate structure and coordinate system

According to Fig. 4, the waveguide structure has three layers, where x = 0 plane is still on the metal interface, and a dielectric film of thickness t is placed on the metal plate. When TM modes propagate in the positive z-direction, the mode field distribution equations can be written as [17]:

$$H_y(x) = \begin{cases} A(\cos h_2 t + \dfrac{h_m \varepsilon_2}{h_2 \varepsilon_m} \sin h_2 t) e^{-h_1(x-t)} & x \geq t \\ A(\cos h_2 x + \dfrac{h_m \varepsilon_2}{h_2 \varepsilon_m} \sin h_2 x) & 0 \leq x \leq t \\ A e^{h_m x} & x \leq 0 \end{cases} \qquad (4)$$

The dispersion equation of TM mode is [17]:

$$\tan h_2 t = \frac{h_2 \varepsilon_m h_1 \varepsilon_2 + h_m \varepsilon_1 h_2 \varepsilon_2}{h_2 \varepsilon_m h_2 \varepsilon_1 - h_m \varepsilon_2 h_1 \varepsilon_2} \qquad (5)$$

where $h_1 = (\beta^2 - n_1^2 k^2)^{1/2}$, $h_2 = (n_2^2 k^2 - \beta^2)^{1/2}$, $h_m = (\beta^2 - n_m^2 k^2)^{1/2}$. Polystyrene (PS) is used as the material of the dielectric film with a parameter of $n_2 = \sqrt{\varepsilon_2} = 1.58 - j0.0036$ [19].

By Eq.(5), we calculate the dependence of loss with respect to film thickness at f = 1 THz and present the corresponding effective refractive index, as shown in Fig. 5:

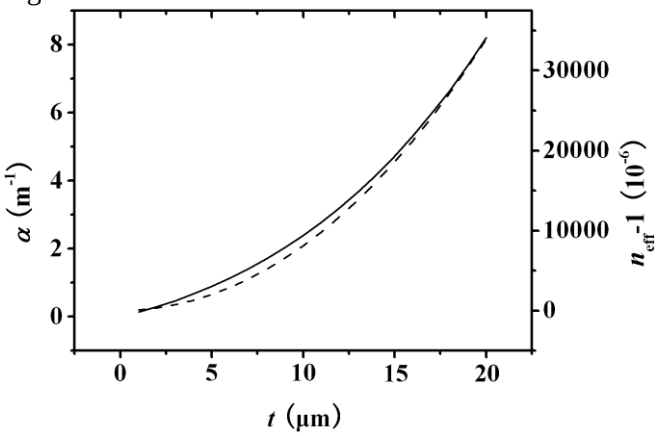

Fig. 5 Variation of loss (solid line) and effective refractive index (dashed line) of coated metal plate as a function of dielectric film thickness at 1 THz.

Figure 5 shows that when there is a very thin dielectric film on the metal plate surface, the loss will be much larger than the case of bare metal plate (such as at film thickness t = 1 μm, the loss is $\alpha = 0.142m^{-1}$ which is two orders of magnitude larger than bare metal plate loss $\alpha = 0.0072m^{-1}$). Loss increases with the increase of film thickness. At the film thickness of t = 20 μm, the loss is $\alpha = 8.20m^{-1}$ which is three orders of magnitude larger than the loss of bare metal plate. At the same time effective refractive index increases as t increases, which indicates that the mode field radius will decrease.

By Eq.(5), we also calculate the dependence of the loss on THz frequency at t = 10 μm and present the corresponding effective refractive index, as shown in Fig. 6:

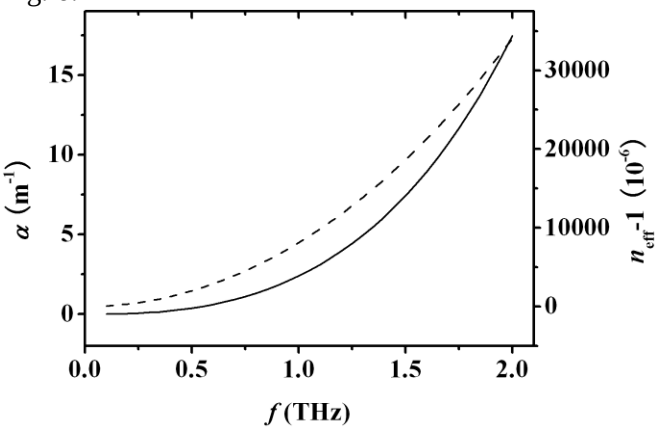

Fig. 6 The dependence of loss (solid line) and effective refractive index (dashed line) of metal plate after coating on THz frequency when t = 10 μm.

Figure 6 shows that the loss increases with the increase of frequency. It is worth to point out that the rate of the effective refractive index changing with the THz frequency is increased by about 5 orders of magnitude than bare metal plate, which indicates that the group velocity dispersion of metal plate increase significantly after coated.

By Eq.(4), we get the mode field distribution for the film thickness t = 20 μm at THz frequency f = 1 THz, as shown in figure 7:

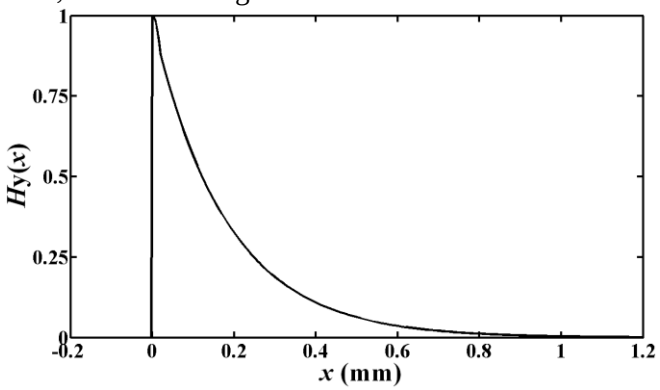

Fig.7 Mode field distribution of metal plate after coating a 20 μm thick film at 1THz

Figure 7 shows that after dielectric coating, the mode field radius (amplitude decay as 1/e) is about 0.2 mm (to further increase film thickness mode field radius will be smaller); However, figure 3 illustrates that the mode field radius of bare metal plate is about 100 mm, which is 500 times larger than coated metal plate. Because of this significant reduction of the mode field radius, energy detection at a distance from metal plate drastically changes after coating the dielectric material.

This sensitivity aspect is useful for the non-destructive evaluation of thin film using THz radiation.

3.2 The coupling of THz SPPs on bare metal plate using mode of dielectric film

As described in reference [12], the thoeretical coupling efficiency of dielectric layer THz surface wave (DL-TSW) using PPWG TEM mode (modified by the dielectric layer) can be as high as 60%. However the coupling efficiency of THz SPPs on bare metal plate is extremely low. We first propose the coupling of THz SPPs on metal plate using mode of dielectric film. The coupling structure is shown in Fig. 8:

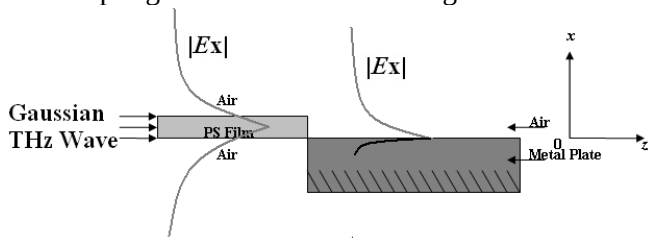

Fig.8 The structure of coupling metal plate THz SPPs using PS film.

The mode field distribution equations of transverse electric field for the incident THz beam from dielectric film on the *x* direction can be derived from Eq. (4) as $E_x = (\beta / \omega\varepsilon)H_y$, and it can be written as:

$$\psi_A(x) = \begin{cases} A(\beta/\omega\varepsilon_1)(\cos h_2 t + \frac{h_1\varepsilon_2}{h_2\varepsilon_1}\sin h_2 t)e^{-h_1(x-t)} & x \ge t \\ A(\beta/\omega\varepsilon_2)(\cos h_2 x + \frac{h_1\varepsilon_2}{h_2\varepsilon_1}\sin h_2 x) & 0 \le x \le t \\ A(\beta/\omega\varepsilon_1)e^{h_1 x} & x \le 0 \end{cases} \quad (6)$$

From Eq. (1) we can write the mode distribution equations of transverse electric field on the metal plate as:

$$\psi_B(x) = \begin{cases} A(\beta'/\omega\varepsilon_1)e^{-h_1' x} & x \ge 0 \\ A(\beta'/\omega\varepsilon_m)e^{h_m x} & x \le 0 \end{cases} \quad (7)$$

The overlap integral on *y* direction is 100%, so the coupling efficiency can be written as [20]:

$$C = \frac{\left|\int_S \psi_A \psi_B^* dS\right|^2}{\int|\psi_A|^2 dS \int|\psi_B|^2 dS} \quad (8)$$

From Eq. (8), we calculate the coupling efficiency as a function of the thickness of the PS film *t* at *f* = 1 THz, as shown in Fig. 9:

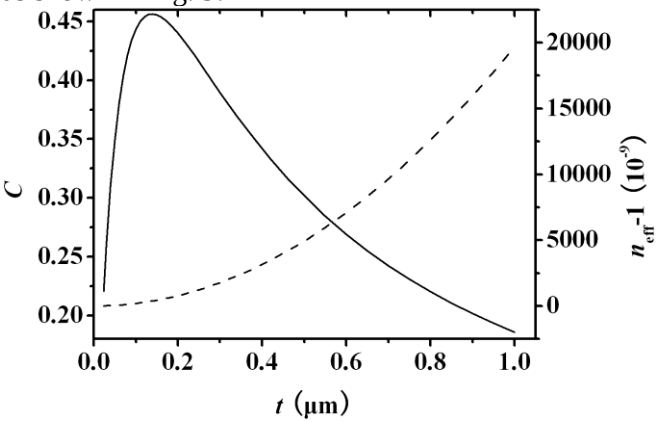

Fig.9 Coupling efficiency (solid line) of metal plate using single PS film mode and effective refractive index of single PS film (dashed line) as a function of film thickness *t* at 1 THz.

By Fig. 9 we can see that there is a maximum coupling efficiency as the thickness of the PS film *t* increases from a very small value to 1 μm. And at *t* = 0.14 μm, the maximum coupling efficiency is 45.64%. When *t* is very close to the minimum thickness (the near zero loss mode cutoff thickness, here *t* = 0.024μm), the mode field radius of the PS film tend to be much bigger than the metal plate and this causes the lower matching degree between the two mode field distributions, so the coupling efficiency is low. When *t* is greater than the optimum thickness, the mode field radius of the PS film decreases and it is far less than the mode field radius of metal plate THz SPPs, which makes the matching degree of the two mode field distribution very low, and hence the coupling efficiency is very low.

This can be seen by the varying of the effective refractive index of the PS film. The effective refractive index increase as *t* increasing which indicates that the mode field radius of the PS film decreases monotonously. The maximum coupling efficiency appears when the effective refractive index of both the PS film and the metal plate are very close and the matching degree of the two mode field distribution is the highest. When *t* = 0.14 μm, the effective refractive index of PS film is $n_{eff} - 1 = 386 \times 10^{-9}$, and the effective refractive index of the metal plate is $n_{eff} - 1 = 156 \times 10^{-9}$.

3.3 The hybrid plasmonic modes of the metal plate with a dielectric slab above

The structure of a dielectric slab placed above metal plate is shown in Fig. 10:

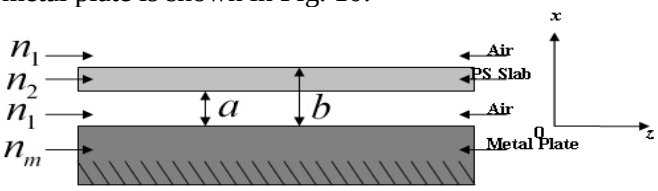

Fig. 10 The structure of dielectric slab placed above the metal plate and the coordinate system

In Fig. 10, *x* = 0 plane is on the metal interface, *a* is the air interval, $t = b - a$ is dielectric slab thickness. The dispersion equation of TM mode is derived as [17]:

$$\tan h_1 a = \frac{\frac{h_3}{\varepsilon_1} + \frac{h_m}{\varepsilon_m} + (\frac{h_3 h_m \varepsilon_2}{h_2 \varepsilon_m \varepsilon_1} - \frac{h_2}{\varepsilon_2})\tan h_2(b-a)}{(\frac{h_2 h_m \varepsilon_1}{h_1 \varepsilon_m \varepsilon_2} + \frac{h_3 h_1 \varepsilon_2}{h_2 \varepsilon_1^2})\tan h_2(b-a) + \frac{h_1}{\varepsilon_1} - \frac{h_3 h_m}{h_1 \varepsilon_m}} \quad (9)$$

where $h_m = (\beta^2 - n_m^2 k^2)^{1/2}$, $h_1 = (n_1^2 k^2 - \beta^2)^{1/2}$, $h_2 = (n_2^2 k^2 - \beta^2)^{1/2}$, $h_3 = (\beta^2 - n_1^2 k^2)^{1/2}$.

By Eq. (9), We calculate the dependence of loss as a function of THz frequency when the air interval *a* = 5 mm and 3 mm at slab thickness *t* = 0.1 mm as shown in Fig. 11:

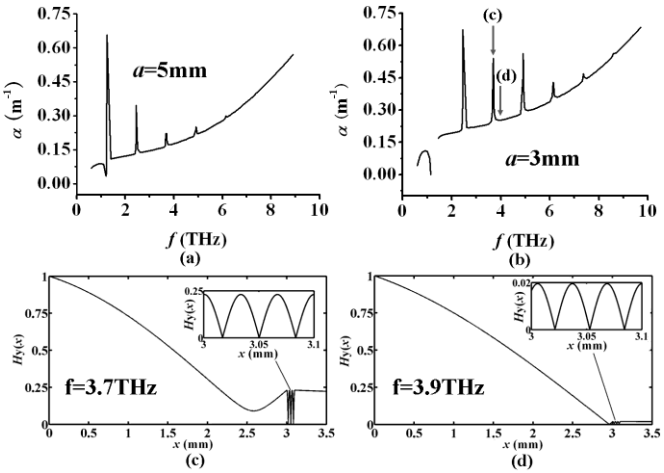

Fig. 11 The dependence of loss on THz frequency after placing a dielectric slab above metal plate, when air interval is a = 5 mm (a) and 3 mm (b). The normalized magnetic field profiles are given at the highest loss point f = 3.7 THz (c) and the lowest loss point f = 3.9 THz (d) for a = 3 mm and mode order n = 3. The insets are magnetic field profiles in the dielectric slab.

Figure 11(a) and 11(b) show that after placing a slab above the metal plate, the transmission spectrum is a combine effect of the slab and the metal plate. On one hand, the THz wave shows anti-resonant reflection on the dielectric slab's surface which appears loss peaks at the resonance frequencies. On the other hand, the basic loss increases monotonously which is predicted by the solid line of Fig. 2. When a certain THz frequency becomes the resonance frequency of the thickness of t = 0.1 mm, the mode appears more energy in the slab (as shown in Fig. 11(c)) with high absorption loss, and the loss spectral appears a sharp peak. However, the loss peaks become much unclearer in the higher frequencies. This tells that the effect of the metal plate is more abvious in the higher frequencies. Figure 11(a) and 11(b) show the loss peaks at 1.24 THz, 2.45 THz, 3.70 THz, 4.91 THz, 6.13 THz, 7.37 THz, 8.58 THz corresponding to the mode order n = 1, 2, 3, 4, 5, 6 and 7, respectively. The resonance frequencies can be calculated by the equation of [21] $f_n = \frac{nc}{2t\sqrt{n_2^2 - 1}}$, where c is the speed of light in vacuum. For the dielectric slab with a thickness of t = 0.1 mm, we get the theoretical resonant frequencies are 1.23 THz, 2.45 THz, 3.68 THz, 4.90 THz, 6.13 THz, 7.36 THz, 8.58 THz corresponding to the mode order n = 1, 2, 3, 4, 5, 6 and 7, respectively. The numerical values agree well with the theoretical values. It is worth to point out that in Fig. 11(b), for the mode order n = 1, there appears a near zero loss cutoff mode and it replaces the anti-resonant reflecting mode of n = 1 for a = 3 mm. However, this behavior is absent for a = 5 mm. As discussed in part 3.2, there is a near zero loss mode cutoff thickness at 1 THz of the single dielectric flim waveguide, and there is also a near zero loss mode cutoff frequency at t = 0.1 mm of the single dielectric slab waveguide. When the loss of the mode tend to zero, the mode field radius tends to infinity. At this time the near zero loss mode cutoff friquency is affected by the metal plate. When a is much larger than the wavelength of the THz wave, the near zero loss cutoff mode is out of the range of THz frequency. Fig. 11(c) and 11(d) show that the mode appears much less energy in the slab at the low loss frequency. The insets reveal that for n = 3, the total phase in the dielectric slab is 3π.

In order to know the effects of air interval between the dielectric slab and the metal plate a, we get the loss spectrum at different a when t = 0.1 mm by calculate Eq. (9) as shown in Fig. 12:

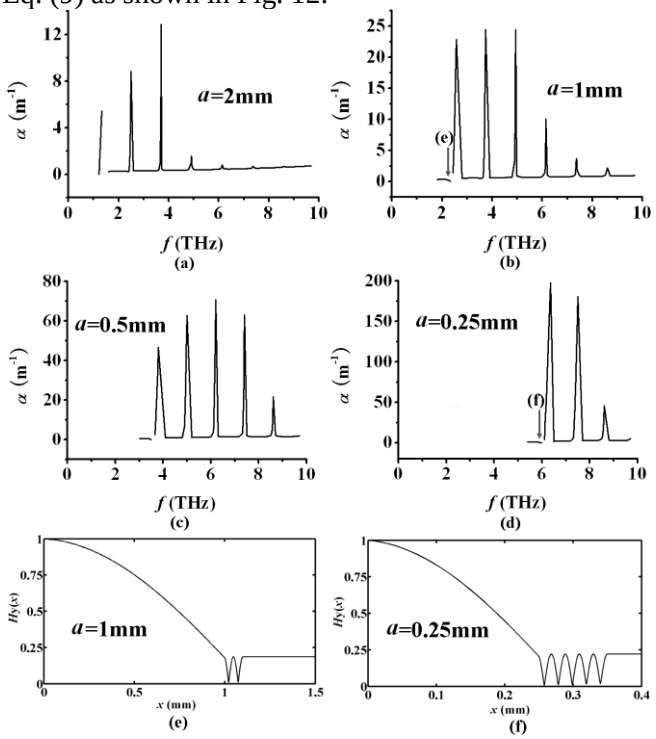

Fig. 12 The dependence of loss on THz frequency after placing a dielectric slab above metal plate, (a) the air interval is a = 2 mm; (b) a = 1mm; (c) a = 0.5 mm; (d) a = 0.25 mm. (e) and (f) are the normalized magnetic field profiles at the near zero loss cutoff mode for a = 1 mm (e) and 0.25 mm (f), repectively.

Figure 12 shows that when a decreases, the effects of the dielectric slab on loss become much more obvious as can be seen that the loss peaks in the higher frequencies become much clearer and the losses at peaks are much larger. At the same time the effect of the metal plate is also very important as can be seen that the near zero loss cutoff mode move to the higher order, and the lower order mode disappears. We can also see that the number of loss peaks decreases when a decreases from a larger value to a very small value.

Actually, when a is small enough, the loss peak will disappear for all modes are cutoff. The resonance frequencies appear a little blue shift as a decreases, but it is negligible. Fig. 12(e) and 12(f) show the field profiles at the near zero loss cutoff mode, which tell us that as a decrease, the total phase in dielectric slab for near zero loss cutoff mode increase. For a = 1 mm, it is about 2π, and for a = 0.25 mm it is about 5π, which reveals that when a = 1 mm and 0.25 mm, the near zero loss cutoff mode replace the anti-resonant reflecting mode of n = 2 and n = 5, respectively. We can also know that the linewidth of the loss peaks becomes narrower in the higher frquencies because the wavelength is smaller.

4. Conclusion

In conclusion, we report the guiding of THz SPPs using metal plate. We theoretically study the transmission characteristics of the bare and dielectric coated metal plate and compared the difference between them. We propose coupling the THz SPPs on bare metal plate using single dielectric film, and the highest theory coupling efficiency we get can be 45.64%. Moreover we study the hybrid plasmonic mode of a dielectric slab above the metal plate, and we find that the THz SPPs on metal plate is strongly affected by the dielectric slab. We further discuss the interesting phenomenon of the transmission spectrum influenced by the variation of the air interval between the dielectric slab and metal plate. We believe that these results are very useful for sensing applications of THz SPPs on metal plate.

References

[1] K.Wang, and D. M. Mittleman, “Metal wires for terahertz waveguiding,” Nature 432, 376 (2004).

[2] C. H. Lai, Y. C. Hsueh, H. W. Chen, Y. J. Huang, H. C. Chang, and C. K. Sun, “Low-index terahertz pipe waveguides,” Opt. Lett. 34(21), 3457–3459 (2009).

[3] D. Gacemi, J. Mangeney, T. Laurtent, J. G. Lampin, T. Akalin, K. Blary, A. Degiron, P. Crozat, and F. Meng, “THz surface plasmon modes on planar Goubau lines,” Opt. Express, 20(8), pp8466-8471, 2012.

[4] C.-H. Lai, B. You, J.-Y. Lu, T.-A. Liu, J.-L. Peng, C.-K. Sun, and H. C. Chang, “Modal characteristics of antiresonant reflecting pipe waveguides for terahertz waveguiding,” Opt. Express 18, 309-322(2010).

[5] E. Nguema, D. Fèrachou, G. Humbert, J. L. Auguste, and J. M. Blondy, “Broadband terahertz transmission within the air channel of thin-wall pipe,” Opt. Lett. 36, 1782–1784 (2011).

[6] T. Jeon, J. Zhang, and D. Grischkowsky, “THz Sommerfeld wave propagation on a single metal wire,” Appl. Phys. Lett., 86(16), pp161904, 2005.

[7] Q. Cao, and J. Jahns, “Azimuthally polarized surface plasmons as effective terahertz waveguides,” Opt. Express, 13(2), pp511-518, 2005.

[8] B. You, J.-Y. Lu, J.-H. Liou, C.-P. Yu, H.-Z. Chen, T.-A. Liu, and J.-L. Peng, “Subwavelength film sensing based on terahertz anti-resonant reflecting hollow waveguides,” Opt. Express 18(18), 19353–19360 (2010).

[9] B. You, J.-Y. Lu, C.-P. Yu, T.-A. Liu, and J.-L. Peng, “Terahertz refractive index sensors using dielectric pipe waveguides,” Opt. Express 20(6), 5858–5866 (2012).

[10] M. Wächter, M. Nagel, and H. Kurz, “Frequency-dependent characterization of THz Sommerfeld wave propagation on single-wires,” Opt. Express 13(26), 10815–10822 (2005).

[11] Nick C. J. van der Valka and Paul C. M. Planken, “Effect of a dielectric coating on terahertz surface plasmon polaritons on metal wires,” Appl. Phys. Lett. 87, pp071106 (2005).

[12] M. Gong, T.-I. Jeon, and D. Grischkowsky, “THz surface wave collapse on coated metal surfaces” Opt. Express 17(19), 17088-17101 (2009).

[13] J. Saxler, J. G. Rivas, C. Janke, H. P. M. Pellemans, P. H. Bolı´var, and H. Kurz, “Time-domain measurements of surface plasmon polaritons in the terahertz frequency range” PHYSICAL REVIEW B 69, 155427 (2004).

[14] T. H. Isaac,W. L. Barnes, and E. Hendry, “Determining the terahertz optical properties of subwavelength films using semiconductor surface plasmons” APPLIED PHYSICS LETTERS 93, 241115 (2008).

[15] R. F. OULTON, V. J. SORGER, D. A. GENOV, D. F. P. PILE AND X. ZHANG, “A hybrid plasmonic waveguide for subwavelength confinement and long-range propagation” nature photonics 2, 496-500 (2008).

[16] M. Z. Alam, J. Meier, J. S. Aitchison, and M. Mojahedi, “Propagation characteristics of hybrid modes supported by metal-low-high index waveguides and bends” Opt. Express 18(12), 12971-12979 (2010).

[17] A. Yariv, Optical Electronics in Modern Communications (Oxford U. Press, Oxford, 2007).

[18] M. A. Ordal, R. J. Bell, R. W. Alexander, Jr, L. L. Long, and M. R. Querry, “Optical properties of fourteen metals in the infrared and far infrared: Al, Co, Cu, Au, Fe, Pb, Mo, Ni, Pd,Pt, Ag, Ti, V, and W.” Applied Optics. 24, 4493-4499 (1985).

[19] J. R. Birch, “The far-infrared optical constants of polypropylene, ptfe, and polystyrene,” Infrared Phys. 33(1), 33–38, (1992).

[20] J.A.Arnaud, Beam and Fiber Optics (Academic Press, 1976).

[21] M. A. Duguay, Y. Kokubun, T. L. Koch, and L. Pfeiffer, “Antiresonant reflecting optical waveguides in SiO2-Si multilayer structures,” Appl. Phys. Lett. 49 (1), 13–15 (1986)